International Archive of Applied Sciences and Technology, Vol 1 [1] JUNE 2010: 10 - 19


ISSN 0976- 4828
http:// www.soeagra.com

ORGINAL ARTICLE

# Electro-hydraulic Anisotropy of Fractures in parts of Abakaliki, Ebonyi State, Nigeria using ARS method

**Odoh, B. I.**
Department of Geological Sciences, Nnamdi Azikiwe University,
P.M.B. 5025 Awka, Anambra State, Nigeria.
Tel: +234-8037240806:
E-mail: lifeaquifer2000@yahoo.co.uk

**ABSTRACT**

*Azimuthal resistivity surveys were used to determine the anisotropic properties of fractures in parts of Abakaliki in Ebonyi State University Nigeria for groundwater development within the area. Measured apparent resistivities varied with the orientation of the array. Graphical interpretation of the azimuthal resistivity data identified fracture systems at depths 28.3, 40.0 and 50.0m. SE orientation ($112.5^0$, $135^0$ and $157.5^0$) are dominant at 40.0m and 50.0m while at depth of 28.3m, orientation varied between N and NE ($0^0$ and $22.5^0$). Coefficient of anisotropy $\lambda$ ranges between 1.23 and 1.44 while fracture porosity varies between 0.02 and 0.09 in the area assuming that anisotropy is due to fracturing. Borehole performance data supports the interpretation of azimuthal resistivity data. Of the 8 pump tested wells within the study area, borehole 8 in the country southeast of the study area showed highest groundwater flow rate of 396 (litres/minute) when compared with other wells in the study area. Result of groundwater head contouring also showed that flow of groundwater in the area is in the SE orientation which possibly could be associated to fracture controlled flow. Fracture mapping of bedrock outcrops at 8 selected sites within the area indicates that the maximum fracture-strike frequency is oriented at $22.5^0$.*

***KEYWORDS:*** *Electrical anisotropy, fractured shale, porosity, permeability, Abakaliki.*

## INTRODUCTION

Fractures in rocks are important pathways for groundwater flow and contaminant migration. Groundwater flow through a fracture network is strongly influenced by hydraulic anisotropy resulting from the geometry of the fractures. The preferential strike of fracture sets makes rock to be both electrically and hydraulically anisotropic, whereas the variation in the size and opening of fractures causes heterogeneity [1]. Azimuthal resistivity surveys (ARS) are conducted to determine the principal direction of electrical anisotropy.

The identification and characterization of fractures is important in rocks with low primary (or matrix) porosity because the bulk porosity and permeability are determined mainly by the intensity, orientation, connectivity, aperture, and infill of fracture systems [2]. The hydraulic conductivity of fracture systems can range over several orders of magnitude.

Azimuthal resistivity surveying has been adopted [3,4,5,2,6,7,1] as a technique for determining the principal directions of electrical anisotropy. Typically, any observed change in apparent resistivity with azimuth is interpreted as invocative of anisotropy (generally fracture anisotropy). It is often assumed that the principal directions of hydraulically conductive fracture measured from electrical anisotropy may be inferred from the measured electrical anisotropy (apparent resistivity ($\rho a$) as a function of azimuth and the strike of the fracture), since both current flow and groundwater are channelled through fractures in the rock. ARS details from electrical anisotropy, sometimes, may not be a proof for hydraulically active fractures as other features may also indicates such anisotropy. For example; clay mineral lining bedrock fractures can also generate electrical anisotropy. Therefore, ARS can fail when structural features other than fractures cause the subsurface to exhibit anisotropy and or heterogeneity. This has resulted in ambiguity in the geologic interpretation of several previous ARS investigations. [4,8].

In this study, we report on the capabilities of azimuthal resistivity survey to (1) to determine the characteristic fracture patterns and porosity of a subsurface fractured shale, (2) compare the determined orientations to those obtained from surface outcrop fracture map within the study area and to (3) integrate the results of selected borehole performance test and groundwater head contouring to provide useful methodology to characterize subsurface fractures.

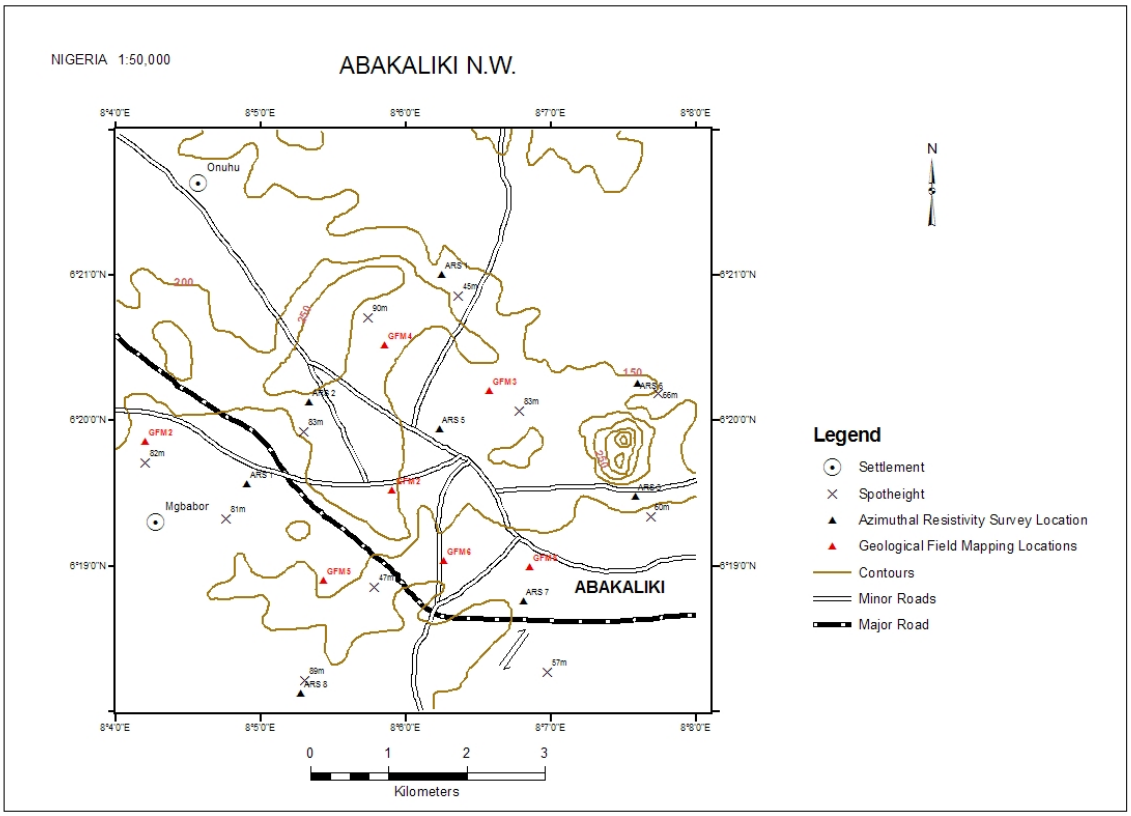


Figure 1: Map of Abakaliki showing the study area

## GEOLOGIC SETTING

Figure 1 shows the location of the study area which covers an approximate area of about 9 km$^2$. The underlying rock in the area is the Abakaliki shale which lies within the Asu River Group of mid Albian age in the Southeastern Nigeria. The Abakaliki shale are poorly bedded, occasionally sandy, and consists of Splintery metamorphosed mudstones. Lenses of sandstone and sandy limestone are highly jointed and fractured.

The geologic history of Abakaliki, is characterized by compressional tectonic stresses. The associated stresses caused metamorphism and fracturing of older marine and volcanic rocks. Primary porosity is low due to geologic conditions. The low primary porosity suggests very poor groundwater transmission and storage capabilities; however, the development of secondary porosity by fracturing and faulting has lead to increase in the bulk permeability of the fractured shale.

Asu River Group was deposited in a shallow marine environment during a transgressive phase [9]. The Albian shale in the area was intruded by younger intrusions, which in combination with the numerous fracture systems have created secondary porosity. The fracture systems which spread across Abakaliki anticlinorium and Afikpo syncline in the Benue rift during the deformational episode originated from vertical movement resulting from the rising and cooling of magma, which intruded the sediments in the Santonian time (Umeji, personal communication, 2005). These shales are the earliest known sediments and lie unconformably on the Basement [10, 9].

## METHOD

To map the orientations of the subsurface fractures at selected sites with very limited rock exposures, resistivity surveys were carried out using the square array method to measure the changes in apparent resistivity with the azimuth. An initial array test selected square array with a $22.5^0$ azimuth step (figure 2) as a suitable array owing to the possession of the following properties:

- **Higher sensitivity**. The step size is confirmed similar to a linear array but sensitivity is higher than dipole array because two MN lines are at $90^0$ differences.
- **Completely identical signals in both MN lines.** This property above anisotropic media allow to measure signs only in one line, hence measurements in two MN lines help to distinguish in homogeneous medium from anisotropic one by taking into account the difference of two signals.
- **Field survey convenience.**

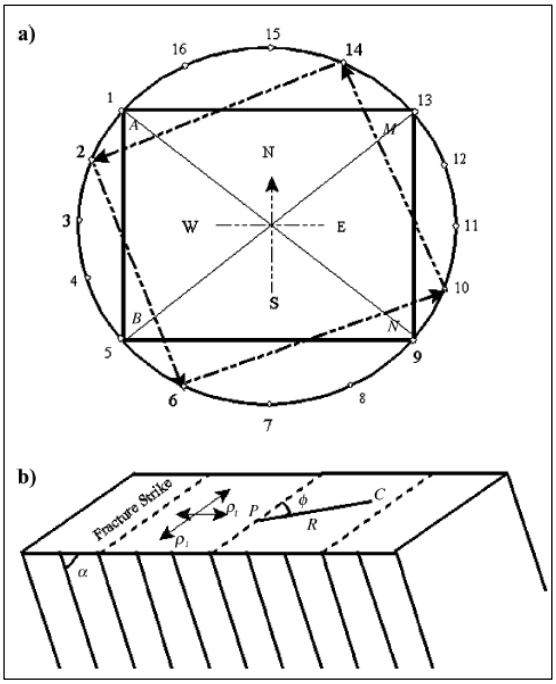


Fig. 2: (a) Electrode arrangement for the square-array azimuthal survey; A, B = current electrodes; M, N = potential electrodes. (b) A homogeneous anisotropic half-space showing the orientation $\Phi$ of current and potential electrodes positions (C and P) with respect to the strike of fractures; **ρ**l is the apparent resistivity measured when measurement electrode are aligned longitudinal (parallel) to the fracture strike, and **ρt** is the traverse alignment of electrodes with respect to fracture strike. The term α is the angle the fracture makes with the vertical [7].

Four azimuthal resistivity surveys were carried out at different locations using the Earth model Res 500. The square array was expanded about a center point, increments of A $(2)^{1/2}$ [11], so the sounding s can be interpreted as a function of depth as indicated from the nature of the array sizes. The apparent resistivity (**ρa**) and the geometric factor (k) for the survey as shown in Table 1 were calculated using equations 1 and 2 respectively.

$$\rho_a = \frac{k\Delta v}{I} \qquad 1$$

$$k = \frac{2\pi A}{2-(2)^{1/2}} \qquad 2$$

where I is the current in amperes and Δv is the voltage change in volts and the resistance is the ration of the voltage to the current.

**Table 1.** Data acquired from the azimuthal resistivity surveys:
ARS1 (Ωm-m)

| A(m) | K | Mean | $0^0$ | $22.5^0$ | $45.0^0$ | $67.5^0$ | $90^0$ | $112.5^0$ | $135^0$ | $157.5^0$ |
|---|---|---|---|---|---|---|---|---|---|---|
| 5.0 | 53.6 | 1103.8 | 825 | 563 | 1,206 | 1,734 | 187 | 1011 | 1,936 | 1,368 |
| 7.1 | 75.8 | 1139.7 | 838 | 269 | 1,089 | 1,776 | 441 | 1,137 | 2431 | 1,137 |
| 10.1 | 107.3 | 2555.8 | 9,687 | 249 | 1,495 | 309 | 1,642 | 1,113 | 4,721 | 1232 |
| 14.1 | 151.7 | 5825.3 | 9,956 | 2,999 | 3070 | 3,659 | 4,042 | 4320 | 3,898 | 3,122 |
| 28.3 | 214.5 | 2053.0 | 2,251 | 1,842 | 2,541 | 2,940 | 1,6830 | 2,340 | 1,400 | 1,427 |
| 40.0 | 429.0 | 1961.6 | 1,420 | 2,146 | 1,574 | 1,923 | 2,950 | 2,464 | 1,680 | 1,536 |
| 50.0 | 536.3 | 2127.5 | 402 | 1,734 | 1,995 | 2,869 | 2,212 | 4,674 | 1,009 | - |

*ARS2 (ohm-m)*

| A(m) | K | Mean | $0^0$ | $22.5^0$ | $45.0^0$ | $67.5^0$ | $90.0^0$ | $112.5^0$ | $135^0$ | $157.5^0$ |
|---|---|---|---|---|---|---|---|---|---|---|
| 5.0 | 53.6 | 805.6 | 1,323 | 697 | 914 | 246 | 649 | 659 | 541 | 1,416 |
| 7.1 | 75.8 | 596.6 | 238 | 248 | 1,096 | 996 | 380 | 716 | 825 | 274 |
| 10.0 | 107.3 | 896.8 | 103 | 204 | 183 | 2,103 | 2,548 | 741 | 450 | 832 |
| 14.1 | 151.7 | 847.6 | 138 | 316 | 1,092 | 1,917 | 518 | 1,061 | 1,491 | 248 |
| 20.0 | 214.5 | 2798.1 | 2,361 | 1,140 | 2,445 | 2,947 | 3387 | 3,754 | 3151 | 2,200 |
| 28.3 | 303.4 | 4139 | 4940 | 3095 | 3884 | 3,771 | 6,622 | 4,385 | 3,155 | 40.0 |
| 40.0 | 429.0 | 2802.5 | 3015 | 2,686 | 3,600 | 4,000 | 2900 | 2,634 | 1,674 | 1,911 |
| 50.0 | 536.3 | 4068.3 | 1783 | - | 2008 | 4,025 | 4,440 | 4,660 | 4,338 | 7,218 |

*ARS 3 (ohm-m)*

| A(m) | K | Mean | $0^0$ | $22.5^0$ | $45.0^0$ | $67.5^0$ | $90^0$ | $112.5^0$ | $135^0$ | $157.5^0$ |
|---|---|---|---|---|---|---|---|---|---|---|
| 5.0 | 53.6 | 1171.8 | 3,003 | 3350 | 2218 | 326 | 80 | 35 | 287 | 75 |
| 7.1 | 75.8 | 796.10 | 2,154 | 1,895 | 985 | 338 | 17 | 252 | 707 | 21 |
| 10.0 | 107.3 | 676.7 | 2,072 | 592 | 751 | 90 | 43 | 875 | 961 | 30 |
| 14.1 | 151.7 | 929.0 | 429 | 394 | 2,003 | 1,613 | 49 | 702 | 2,200 | 42 |
| 20.0 | 214.5 | 1007.1 | 70 | 2,383 | 3,687 | 403 | 36 | 890 | 558 | 30 |
| 28.3 | 303.4 | 1835.1 | 2,251 | 1,891 | 2,470 | 1,939 | 1,700 | 1,460 | 1,330 | 1,640 |
| 40.0 | 429.0 | 2364.1 | 2,913 | 1,989 | 3,001 | 2,270 | 2,400 | 2,142 | 1,604 | 2604 |
| 50.0 | 536.3 | 2178.3 | 2,336 | 3,842 | 2,095 | 1,770 | 2,160 | 1,590 | 1,783 | 1,850 |

*ARS4 (ohm-m)*

| A(m) | K | Mean | $0^0$ | $22.5^0$ | $45^0$ | $67.5^0$ | $90^0$ | $112.5^0$ | $135^0$ | $157.5^0$ |
|---|---|---|---|---|---|---|---|---|---|---|
| 5.0 | 53.6 | 299.6 | 427.1 | Building obstruction | 252.5 | Building obstruction | 441.1 | Building obstruction | 77.7 | Building obstruction |
| 7.1 | 75.8 | 552.2 | 743.6 | | 648.1 | | 500.3 | | 316.8 | |
| 10.0 | 107.3 | 578.9 | 974.3 | | 1097.7 | | 1113.8 | | 131.0 | |
| 14.1 | 151.7 | 1974.6 | 344.4 | | 679.1 | | 215.4 | | 189.6 | |
| 20.0 | 214.5 | 693.9 | 394.7 | | 1673.1 | | 626.3 | | 81.51 | |
| 28.3 | 303.4 | 1529.1 | 1673.1 | | 626.3 | | 81.51 | | 28.3 | |
| 40.0 | 429.0 | 3668.5 | 3063.1 | | 4405.8 | | 3883.6 | | 3321.3 | |
| 50.0 | 536.3 | 2291.5 | 1911.3 | | 3002.0 | | 2751.6 | | 1501.6 | |

To minimize possible overburden effects, the data were analyzed by plotting the apparent resistivity against azimuths of 28.3, 40.0 and 50.0m A –spacing.

**FRACTURE POROSITY**

Secondary porosity or fracture porosities associated with tectonic fracturing of rocks were estimated using the expression derived by Lane et al. (1995) equation 3;

$$\phi_f = \frac{3.41\times10^4(N-1)(N^2-1)}{N^2C(\rho_{a\max}-\rho_{a\min})} \quad (3)$$

$$N = [(1+\lambda^2-1)\sin^2\alpha]^{1/2} \quad (4)$$

$$\lambda = (\rho_{aT}/\rho_{aL})^{1/2} \quad (5)$$

Where Φ is the strike of the fractures; $\Phi_f$ = fracture porosity; N is the vertical anisotropy related to the co-efficient of anisotropy λ and dip of the bedding plane α as shown in equation (4) $\rho_{a\max}$ = max *imium* apparent resistivity; $\rho_{a\min}$ = minimum apparent resistivity; $\rho_T$ and $\rho_L$ are, respectively, the apparent resistivity transverse and longitudinal to the direction of the fracturing; and C = specific conductance of ground water in microsiemens per centimeter (μs/cm). In this study, the specific conductance of groundwater in the Abakaliki shale averaged 736 μs/cm [12].

**Table 2**: characteristics fracture parameters at each site obtained from analysis of azimuthal resistivity data obtained from the study area

| Locations and coordinates | A – spacing (m) | Major strike direction | Coefficient of anisotropy (λ) | Mean resistant (Ωm) | $\phi_f$ from ARS |
|---|---|---|---|---|---|
| CHS EBSU: ARS 1 | 20.0 | $(22.5^0$(NW-SW)) | 1.23 | 3599.4 | 0.002 |
| | 28.3 | $157.5^0$ (NW-SE) | 1.44 | 2048.3 | 0.009 |
| | 40.0 | $0^0$(N-S) | 1.43 | 2046.7 | |
| Abakaliki High School: ARS 2 | 20.0 | $22.5^0$(NE-SW) | 1.41 | 2068.7 | |
| | 28.3 | $22.5^0$(NE-SW) | 1.46 | 4527.2 | |
| | 40.0 | $157.5^0$(NE-SE) | 1.45 | 2764.8 | 0.004 |
| CAS EBSU: ARS 3 | 28.3 | $135^0$(NW-SE) | 1.36 | 1812.5 | |
| | 40.0 | $135^0$ (NW-SE) | 1.37 | 2193.9 | |
| | 50.0 | $112.5^0$(NW-SE) | 1.55 | 2471.6 | 0.030 |
| Presbyterian Church Kpiri-Kpiri : ARS 4 | 28.3 | $0^0$(N-S) | 1.29 | 1550.2 | 0.0021 |
| | 40.0 | $135^0$(NW-SE) | 1.15 | 3825.3 | |
| | 50.0 | $135^0$(NW-SE) | 1.41 | 2123.2 | 0.026 |

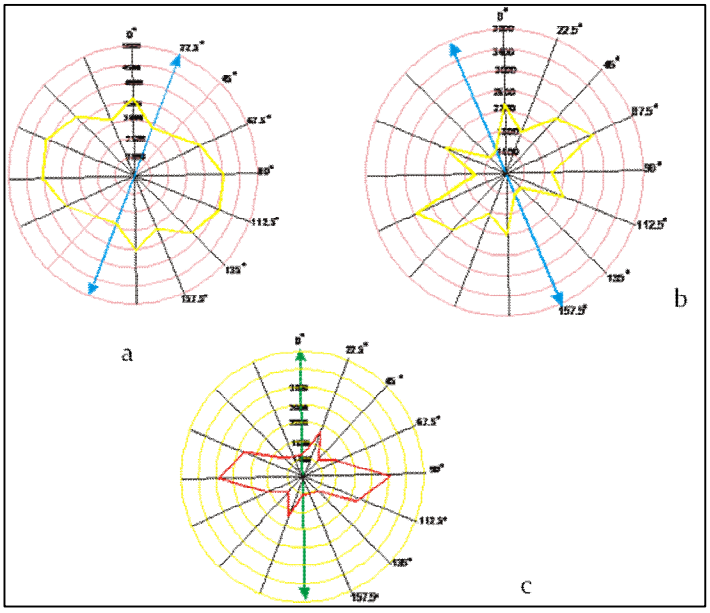


Figure 3a: ARSI polar plots of the apparent resistivity against azimuth at depths:(a) =28.3m, (b) = 40.0m (c) =50.0m

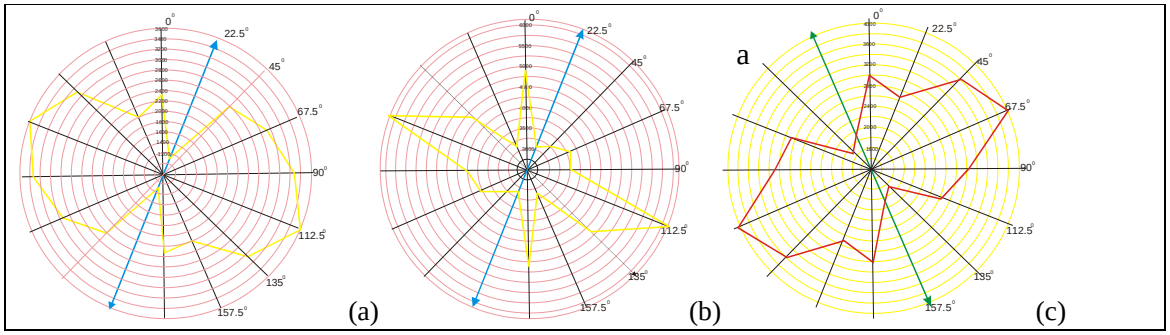


Figure 3b: ARS2 polar plots of the apparent resistivities against azimuths at depths: (a): 28.3m (b): 40.0m (c): 50.0m

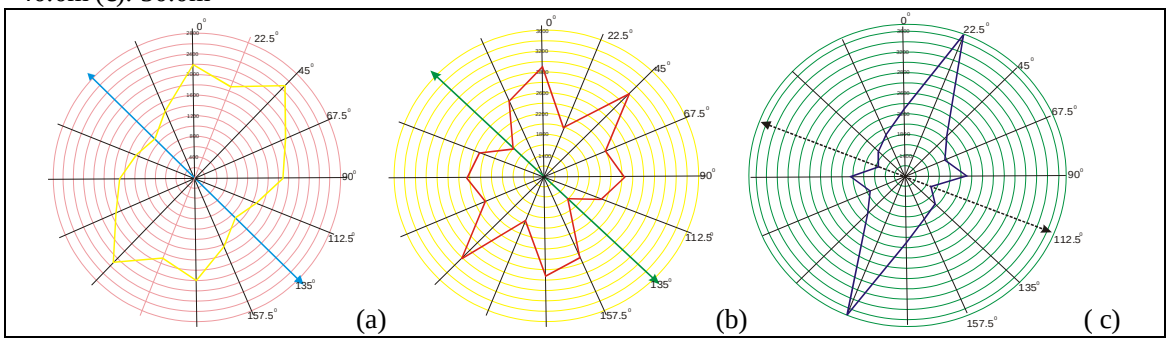


Figure 3c: ARS2 polar plots of the apparent resistivities against azimuths at depths: (a): 28.3m (b): 40.0m (c): 50.0m

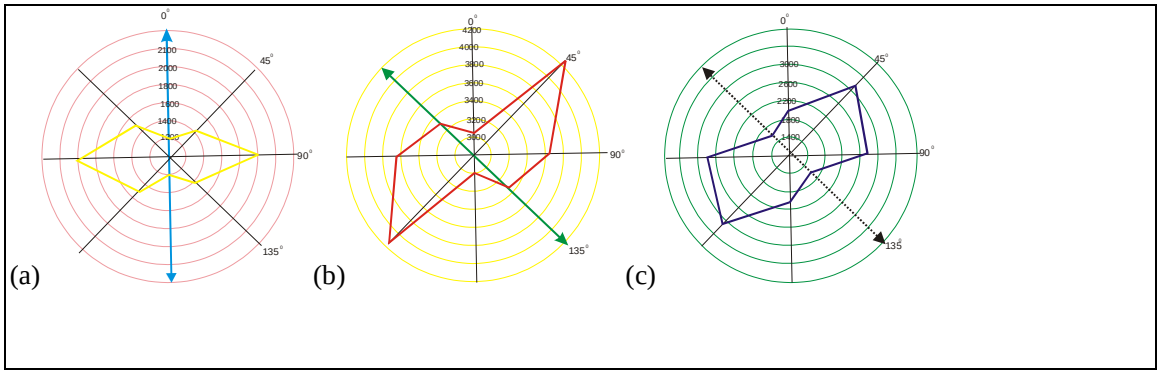


Figure 3d: ARS3 polar plots of the apparent resistivities against azimuths at depths: (a): 28.3m (b): 40.0m (c): 50.0m

## DISCUSSION OF RESULTS

Figure 3 (a)-(d) show the polar plots for the variation of ρa data with azimuths at depths 28.3m, 40.0m and 50.0m. The observed changes in the apparent resistivity were interpreted as an indicator of fracture anisotropy. The fracture strikes at different depths are indicated as an arrow pointed at both ends.Fracture strikes were identified to be perpendicular to the direction of maximum apparent resistivities [13]. The survey identified three fracture systems at 28.3, 40.0 and 50.0m. NW-SE trends are dominant at 40.0m and 50.0m while at depth of 28.3m, trends varied between NE-SW and N-S. These trends are consistent with the dominant orientation of structure found in rock exposures within the Abakaliki shale.

## COMPARISION OF INTERPRETED ARS DATA AND OTHER SUPPORTING DATA

Near the study locations are close outcrops with structural units. These exposed shale outcrops were mapped, which included measurements of strike, dip direction of geologic formations as well as individual fracture planes. The graphically interpreted fracture strike from ARS data of $22.5^0$

correlates well with the fracture-strike frequency data measured at the 8 outcrops. Figure 4 is a histogram showing the distribution of fracture strike with azimuth for the entire area. Figure 5 also shows the polar plots of the mapped fracture orientation on exposed outcrop. The dominant fracture strikes are clearly indicated.

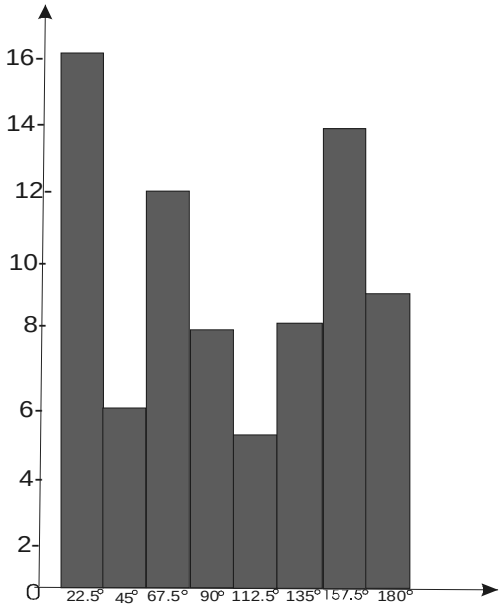


Fig. 4: Histogram showing fracture strike distribution with respect to azimuth

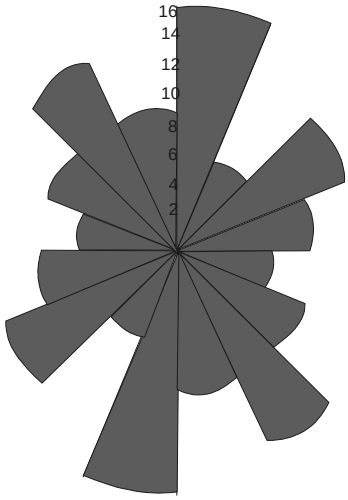


Fig. 5: Polar plots of fracture strike measured at exposed outcrops in the study area

**(a) Groundwater hydraulic head Contouring and visualization**

To further support the interpretation of the azimuthal resistivity data, groundwater hydraulic head data in 12 boreholes and 11 hand dug wells were collected and used to generate the groundwater flow contour map below. The contour map shows the various directions of groundwater flow obtained from the contouring and visualization. Figure 6 establishes the dominant direction of groundwater flow in the area to be in the orientation of SE.

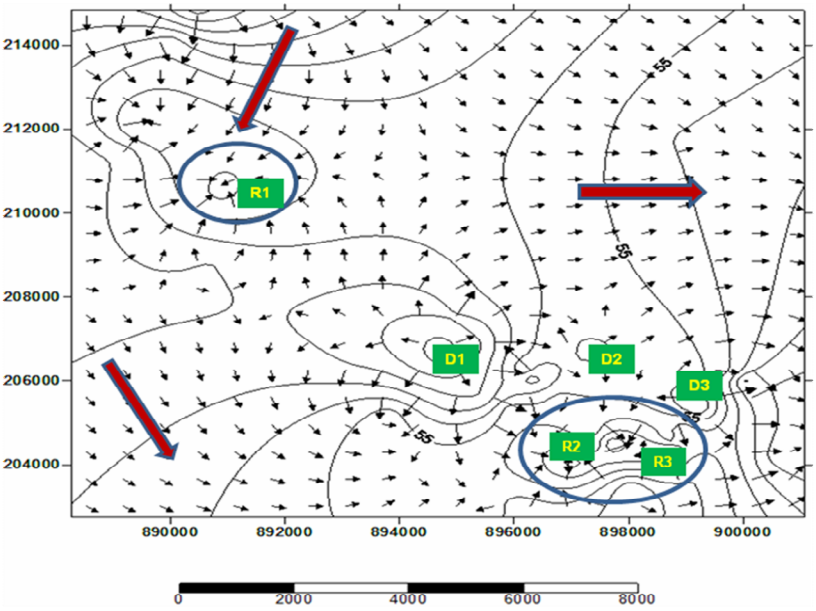


Figure 6: R1, R2, R3 indicate recharge zones; D1, D2, D3 indicate discharge zones while the red arrow show flow directions of groundwater

**(b) Borehole performance test**

Well pumping test was also carried out on the same wells that were contoured to establish if a correlation exist between well yield, and trend of fracturing. One well in the country south of the study area show better yield than any other well in the study area indicating that flow to the well is controlled by fracture flow. Table 3 and figure 7 show the drawdown data and curve generated from the pumping test carried. Other pump test well data are not presented as their yields are significantly lower than well yield of figure 7.

**Table 3**: Drawdown table for a pumped borehole in the south-eastern part of the study area

| Elapsed Time (minutes) | Clock Time | Water Depth(m) | Flow Rate(litres per minute) | Drawdown (m) | Water Colour/Quality |
|---|---|---|---|---|---|
| 0 | 8:30am | 8.00 (SWL) | 0 | 0 | |
| 5 | 8:35am | 8.10 | 99 | 0.6 | Muddy |
| 10 | 8:40am | 8.30 | 136 | 1.2 | Muddy |
| 15 | 8:45am | 8.40 | 173 | 1.8 | Muddy |
| 20 | 8:50am | 8.50 | 211 | 2.4 | Muddy |
| 30 | 9:00am | 8.70 | 248 | 3.0 | Muddy |
| 40 | 9:10am | 8.80 | 285 | 3.6 | Muddy |
| 50 | 9:20am | 9.00 | 322 | 4.5 | Light brown |
| 60 | 9:30am | 9.20 | 359 | 5.5 | Light brown |
| 90 | 10:00am | 9.50 | 396 | 6.4 | Light brown |
| 120 | 10:30am | 9.75 | 396 | 7.2 | Clear-some silt |
| 150 | 11:00am | 10.00 | 396 | 7.8 | Clear-some silt |
| 180 | 11:30am | 10.00 | 396 | 8.2 | Clear |
| 210 | 12:00pm | 10.15 | 396 | 8.8 | Clear |
| 240 | 12:30pm | 10.15 | 396 | 8.8 | Clear |
| 270 | 1:00pm | 10.15 | 396 | 8.8 | Clear |
| 300 | 1:30pm | 10.15 | 396 | 8.8 | Clear |

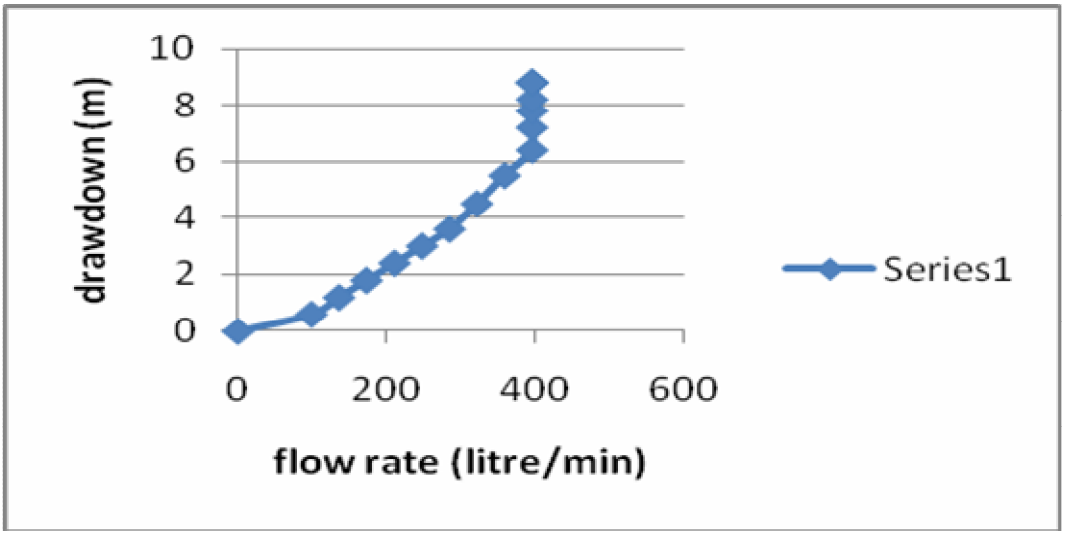


Fig. 7: shows the curve generated from the pump test data. From the curve, at 396 litres per minute, the water level in the borehole continues to drawdown, indicating that the production capacity of the borehole has been exceeded.

The fracture trends obtained from the measurements of azimuthal surveys and exposed outcrop mapping are plotted on the map of the study area to obtain an inferred structural orientation map of the study area as shown in figure 8 below.

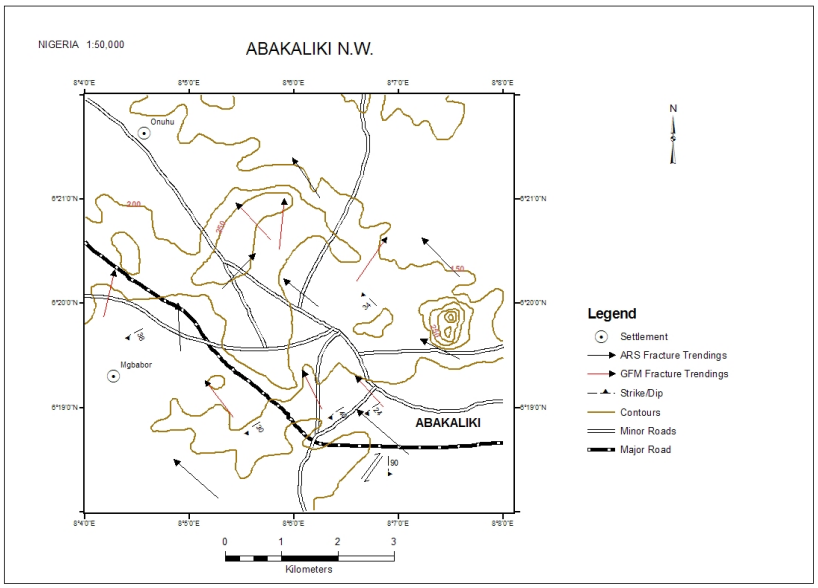


Fig. 8: Measured and inferred structural trends from both azimuthal and geological field mapping.

## CONCLUSIONS

The following conclusions have been deduced from this study:

1. Fracture intensity and density is more in the country NW and SE(mainly in $135^0$ orientation) of the study area, suggesting higher porosity hence, groundwater storage and transmission capability are better in those parts of the study area.
2. The axial trend of the Abakaliki anticlinoria is NW- SE. This conforms to the fracture trends predicted from ARS. These closely match the orientation of dominant fracture trend ($112.5^0$-$157.5^0$) from geologic field mapping in some outcrop around the study area
3. Values of fracture porosity and coefficient of anisotropy are higher in the southern part of the study area. This also correlates very well with the borehole yield data obtained in the same area.
4. Net groundwater flow in the area is controlled by dominant fracture direction. This supports the ARS results obtained in the area.

## REFERENCES

[1] Slater L.D., Wishart D. N., and Gates, E.A. (2006) Self potential improves characterization of hydraulically-active fracture from azimuthal geoelectrical measurements, Geophysical Research Letter.33, L17314

[2] Skyernaa, L., and Jorgensen, N.O. (1993) Detection of local fracture systems by azimuthal resistivity surveys: example from south Norway: Memoirs of the 24th congress of International Association of Hydrogeologists 662 – 671.

[3] Leonard- Mayer P.J. (1984) A Surface resistivity method for measuring hydrologic characteristics of jointed formations, U.S. Bur. mines Report of Investigations 8901.

[4] Taylor, R, W., and Fleming, A.H. (1988) Characterizing jointed systems by azimuthal resistivity surveys, Groundwater 2, 464-474.

[5] Ritzi, R.W., and Andolsek, R.H. (1992) Relation between anisotropic transmissivity and azimuthal resistivity surveys in shallow fractured carbonate flow systems, Ground water, 30, 774-780.

[6] Al Hagrey, S.A., (1994) Electric study of fracture anisotropy at Falkenberg, Germany; Geophysics. 59, 881-888.

[7] Boadu, F.k., Gyamfi, J. and Owusu,E. (2005) Determining subsurface fracture characteristics from azimuthal resistivity survey: A case study at Nsawam, Ghana, Geophysics, 70, B35-B42.

[8] Watson, K.A. and Barker, R.D. (1999) Differentiating anisotropy and lateral effects using azimuthal resistivity Offset wenner Soundings, Geophysics, 64, 749-745.
[9] Reyment, R.A. (1965) Aspect of the Geology of Nigeria, Ibadan University Press. 145p
[10] Burke, K., Dessvaugie, T.F.W., and Whiteman, A.J. (1972) Geological History of Benue Valley and Adjacent Areas: In Burke and Whiteman (eds.): African Geology, University of Ibadan Nigeria.
[11] Habberjam G. M., and Watkins, G.E. (1967) The use of square configuration in resistivity prospecting, Geophysical prospecting 15, 445-467.
[12] Eze, 2008, Chemical analysis of groundwater in parts of Abakaliki, Undergraduate B.Sc. Project, Department of Industrial Chemistry EBSU, 66p.
[13] Keller, G. V., and Frischknecht, F.C. (1966) Electrical Methods in Geophysical Prospecting, Pergamon Press. Inc.
[14] Lane J. W., Jr, Haeni F.P., and Watson, W.M. (1995) Use of a square-array direct current resistivity method to detect fractures in crystalline bedrock in Newhamphere. Groundwater 33, 476-485.